

# Cooperativity, connectivity, and folding pathways of multidomain proteins

Kazuhito Itoh\* and Masaki Sasai

Department of Computational Science and Engineering, Nagoya University, Nagoya 464-8603, Japan

Edited by José N. Onuchic, University of California at San Diego, La Jolla, CA, and approved July 11, 2008 (received for review May 9, 2008)

**Multidomain proteins are ubiquitous in both prokaryotic and eukaryotic proteomes. Study on protein folding, however, has concentrated more on the isolated single domains of proteins, and there have been relatively few systematic studies on the effects of domain–domain interactions on folding. We here discuss this issue by examining human  $\gamma$ D-crystallin, spore coat protein S, and a tandem array of the R16 and R17 domains of spectrin as example proteins by using a structure-based model of folding. The calculated results consistently explain the experimental data on folding pathways and effects of mutational perturbations, supporting the view that the connectivity of two domains and the distribution of domain–domain interactions in the native conformation are factors to determine kinetic and equilibrium properties of cooperative folding.**

energy landscape theory | structure-based model | circular permutation

Our understanding of protein folding has been deepened by the combined efforts of experimental, theoretical, and computational studies of the last decade. Energy landscape theory describes folding as the stochastic relaxation process on the free energy surface of conformational change, where the free energy surface is determined by the compromise of conformational entropy of the polymer chain and interaction energies to stabilize the native conformation (1–3). Because proteins can fold when interactions that stabilize the native conformation dominate over the nonnative interactions that may trap the chain into the irrelevant structures, protein folding can be approximately simulated by using the interaction potentials that are derived from the knowledge of the native structure. With such structure-based models, folding of various small proteins has been simulated, and quantitative agreement between simulations and experiments has been reported (3). The agreement has been improved by simulations that further take account of the residue-dependent energetic differences (4), the atomistic packing (5–7), or the hydration structure (8), and such agreement has convinced us that the topology of the native structure is the primary determinant of the equilibrium and kinetic features of folding at least for small proteins (3) although the atomistic details perturb those features or they sometimes change the delicate balance among folding pathways (9, 10).

These intensive studies on folding have been predominantly focused on small, single-domain proteins or isolated single domains of larger proteins. More than 70% of eukaryotic proteins, however, are composed of multiple domains, and hence we should ask whether the principles of folding found in single domains of proteins also apply to connected multidomain proteins as well (11). Anticorrelation between the contact order and the folding rate has been observed in multidomain proteins (12), and the structure-based simulations on multidomain proteins such as the ankyrin family (13–15) and CV-N (16) have provided consistent results with experiments. The importance of interactions between domains in determining the folding behavior of repeat-containing proteins has been shown theoretically (15). These observed and simulated data suggest the decisive importance of topology of the native structure for folding kinetics in multidomain proteins, but more should be investigated to clarify

how the topology determines the kinetic features. For example, when isolated individual domains that can fold and unfold independently of other domains are connected to a multidomain protein, domains would still behave independently or behave cooperatively through the domain–domain interactions. Although both cooperative folding and independent folding of domains have been observed (11), whether topology determines the cooperativity has not yet been clarified. To shed light on this problem, we here analyze the folding of the example proteins human  $\gamma$ D-crystallin (17–22), protein S (23, 24), and a tandem array of the R16 and R17 domains of spectrin (25–28) by using a simple structure-based model and show that the model indeed captures the essential features of the folding of these multidomain proteins.

Cooperativity of folding should be intrinsically related to the connectivity of the chain. When two regions in a small, single-domain protein approach each other with the native-like steric arrangement to interact as in the native conformation, then the chain connecting these two regions should have more chance to take the native-like configuration. Similarly, when the chain connecting them is native-like, the two regions have more chance to interact to stabilize the native-like configuration. This should lead to a higher probability of realization of two states: the state in which two interacting regions and the chain connecting them are both native-like and the state in which neither two regions nor the chain are native-like. This is the cooperativity arising from the connectivity of the chain. With this cooperativity, the residues that have the native-like configuration should tend to form contiguous domains in the sequence in the course of folding, and such tendency has been highlighted by the structure-based, coarse-grained models of folding (29–39). Success of these models in describing kinetic features of various small proteins showed that connectivity is an important factor to determine the cooperativity. In a similar way, we may expect that the linker region of the chain between two domains and the domain–domain interactions should decide the cooperativity of folding of the connected two domains. In this article, we explore the relation between the cooperativity and connectivity in multidomain proteins by using a structure-based, coarse-grained model.

## Results

**Description of Free Energy Landscape.** As a coarse-grained variable, using  $m_i = 1$  or 0, which represents the configuration at the  $i$ th residue, is convenient:  $m_i$  takes unity when two dihedral angles of the backbone at the  $i$ th residue are within some narrow range around values in the native state conformation and zero other-

Author contributions: K.I. and M.S. designed research; K.I. performed research; K.I. contributed new reagents/analytic tools; K.I. and M.S. analyzed data; and K.I. and M.S. wrote the paper.

The authors declare no conflict of interest.

This article is a PNAS Direct Submission.

\*To whom correspondence should be addressed. E-mail: kazuhito@tbp.cse.nagoya-u.ac.jp.

This article contains supporting information online at [www.pnas.org/cgi/content/full/0804512105/DCSupplemental](http://www.pnas.org/cgi/content/full/0804512105/DCSupplemental).

© 2008 by The National Academy of Sciences of the USA



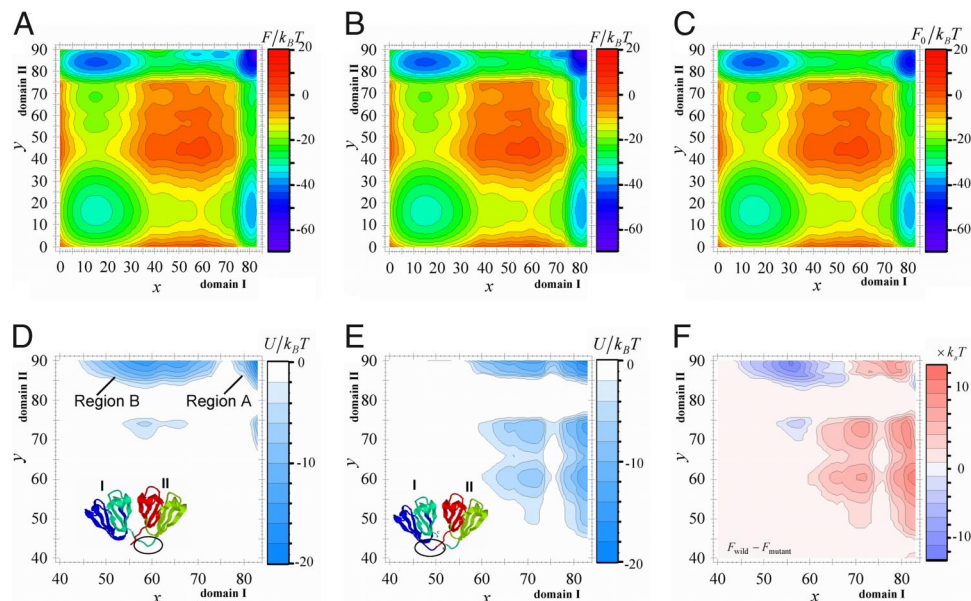


**Fig. 2.** Free energy profiles of H $\gamma$ D-Crys. (A) Free energy surface,  $F(x, y)$  for the wild type. (B)  $F(x, y)$  for the circular permuted. (C) The free energy surface of noninteracting two domains,  $F_0(x, y)$ , where  $x(y)$  is the number of residues that take the native configuration in domain I(II). (D) The differences in free energy between the connected two-domain protein and the separated two noninteracting domains,  $U(x, y)$ , for the wild type. (E)  $U(x, y)$ , for the circular permuted. (F) The difference in free energy between the wild type and the mutant,  $F_{\text{wild}} - F_{\text{mutant}} = \varepsilon/k_B T = 0.53$  and  $\sigma = 1.5k_B$ .

mediate state that has the unstructured domain I and the native-like structured domain II (18–22).

We define order parameters  $x$  and  $y$  by regarding a midpoint in the linker region as the domain boundary with  $n_I = 83$  and  $n_{II} = 90$ . With this definition of two domains, the free energy landscape,  $F(x, y)$ , for  $\varepsilon/k_B T = 0.53$  is drawn in Fig. 2A.  $F(x, y)$  has four distinct minima, which correspond to the native state  $N_I N_{II}$  at  $(x, y) \approx (83, 90)$ , the unfolded state  $U_I U_{II}$  around  $(x, y) \approx (15, 15)$ , and two partially folded states,  $U_I N_{II}$  at  $(x, y) \approx (15, 85)$ , and  $N_I U_{II}$  at  $(x, y) \approx (80, 15)$ . Corresponding to two partially folded states, there are two folding pathways: Pathway I ( $P_I$ ) is the route in which domain I folds first as  $U_I U_{II} \rightarrow N_I U_{II} \rightarrow N_I N_{II}$ , and Pathway II ( $P_{II}$ ) is the route in which domain II folds first as  $U_I U_{II} \rightarrow U_I N_{II} \rightarrow N_I N_{II}$ . The barrier height of the transition  $U_I N_{II} \rightarrow N_I N_{II}$  in  $P_{II}$  is  $\approx 3k_B T$  lower than that of the transition  $U_I U_{II} \rightarrow N_I U_{II}$  in  $P_I$ , whereas  $N_I U_{II} \rightarrow N_I N_{II}$  in  $P_I$  and  $U_I U_{II} \rightarrow U_I N_{II}$  in  $P_{II}$  have almost the same barrier height, so  $P_{II}$  is the dominant pathway with the largest folding rate and  $U_I N_{II}$  is the dominant on-pathway kinetic intermediate. This result agrees with the observed data on the features of the kinetic intermediate state (18–21).

As explained in *Methods*, the influence  $q_i(x, y)$  of the perturbation of interactions on free energy can be used as a structural order parameter of the  $i$ th site under the constraint of  $(x, y)$ . In Fig. 3,  $q_i(x, y)$  at minima  $(x, y) = (15, 85)$  and at four points around saddles  $(x, y) = (50, 85)$ ,  $(58, 87)$ ,  $(68, 87)$ , and  $(75, 87)$  of the free energy surface are shown to describe how the structure is formed along  $P_{II}$ . As shown in Fig. 3, structure of the C-terminal half of domain I (Cth-I) develops after the completion of the structure formation of the C-terminal half of domain II (Cth-II). In this way, the folded domain II catalyzes folding of Cth-I, which then catalyzes the folding of the N-terminal half of domain I (Nth-I). The linker also should be noted to be unstable when domain I is entirely folded at  $(x, y) = (75, 87)$ , whereas it is stable when only Cth-I is folded. This result shows that the linker has an important role in the kinetic process of folding of domain I, whose structural fluctuation is closely associated with fluctuation of domain–domain interactions.

Also notable in Fig. 2A is the existence of an additional free energy valley at approximately  $(x, y) \approx (65, 85)$ . The last step of

folding, the formation of Nth-I catalyzed by the structured Cth-I, is the transition from this free energy valley to  $N_I N_{II}$ . Existence of this additional free energy valley agrees with the experimental data for an intermediate state residing in between  $U_I N_{II}$  and  $N_I N_{II}$  (21). The low free energy valley in  $F(x, y)$  at around the native state extends toward the smaller  $x$ , indicating that the native state has the larger conformational fluctuation at Nth-I. This result is consistent with the observed large  $B$ -factor at Nth-I in the crystal structure.

Asymmetry of  $P_I$  and  $P_{II}$  implies that domains I and II are not independent of each other but fold in a cooperative way. This can be clarified by comparing  $F(x, y)$  with  $F_0(x, y)$  and  $U(x, y)$ . Because each of the two domains undergoes the two-state folding transition, the free energy surface  $F_0(x, y)$  of noninteracting two domains is a composite of two of the two-state transitions and thus has four distinct minima as shown in Fig. 2C.  $P_I$  and  $P_{II}$  in this case have an identical folding rate by definition.  $U(x, y)$  has negative values at around  $N_I N_{II}$  (Region A in Fig. 2D), showing that the domain–domain interactions stabilize the native conformation.  $U(x, y)$  has large negative values at approximately  $y \approx 85$  and  $50 < x < 70$  (Region B in Fig. 2D), which is the region around the free energy saddle in  $F_0(x, y)$ . The free energy of the barrier region of the transition  $U_I N_{II} \rightarrow N_I N_{II}$  in  $P_{II}$  is, therefore, lowered by domain–domain interactions. The lowering of the free energy along  $U_I N_{II} \rightarrow N_I N_{II}$  by 5 to  $10k_B T$  ( $\approx 10$  to  $20\varepsilon$ ) than  $U_I U_{II} \rightarrow N_I U_{II}$  gives rise to the dominance of  $P_{II}$  over  $P_I$ . In this way, the domain–domain interactions contribute to the stability of the native structure in Region A and catalyze the folding process in Region B. Because  $U(x, y)$  is almost zero along  $U_I U_{II} \rightarrow U_I N_{II}$ , the model explains the observed data that the mutations that weaken the domain–domain interactions do not affect the folding rate of domain II although they lower the folding rate of domain I (20, 21).

As shown in Fig. 1A, two domains of H $\gamma$ D-Crys associate almost symmetrically around a twofold axis. Asymmetry of  $U(x, y)$  arises not from this symmetrical distribution of native contacts but from the asymmetrical chain connectivity. As shown in Fig. 1A, domain–domain interactions are formed mainly between Cth-I and Cth-II, whereas domains are connected from

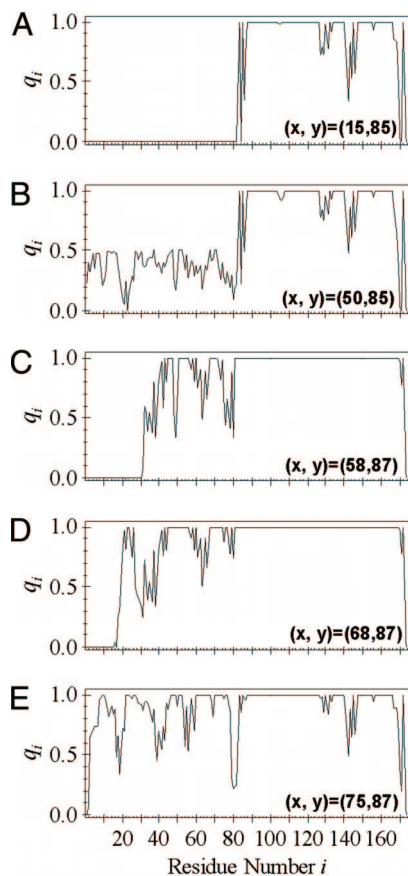


**Fig. 3.** Structure formation of H $\gamma$ D-Crys along the  $U_I N_{II} \rightarrow N_I N_{II}$  process. Structural order parameters  $q_i(x, y)$  for each residue at (A)  $(x, y) = (15, 85)$ , (B)  $(x, y) = (50, 85)$ , (C)  $(x, y) = (58, 87)$ , (D)  $(x, y) = (68, 87)$ , and (E)  $(x, y) = (75, 87)$  for  $\epsilon/k_B T = 0.53$ .

Cth-I to the N-terminal half of domain II (Nth-II). Because the native-like interactions between the two regions are formed with a higher probability when the chain connecting them is native-like, the domain–domain interactions are stabilized when the region from Cth-I through Cth-II becomes native-like. This is the reason why domain II folds first and catalyzes the folding of Cth-I. Thus, the chain connectivity is the origin of asymmetry of  $U(x, y)$ .

For single-domain proteins, the importance of chain connectivity has been examined by circular permutation (40, 41). Here, we point out that circular permutation also should highlight the effects of connectivity in multidomain proteins: As illustrated in Fig. 1B, we may cut the linker between the 83rd and the 84th residues and connect the N terminus of domain I and the C terminus of domain II without changing the native contacts in the model. We here use the same domain name as in the

wild-type protein: The C(N)-terminal domain of the circular permutant is called domain I(II). To stabilize domain–domain interactions in this case, the connected region composed of domain I and Cth-II should be native-like, and hence domain I should fold first.  $F(x, y)$ ,  $U(x, y)$ , and the difference in free energy between the wild type and the mutant,  $F_{\text{wild}} - F_{\text{mutant}}$ , are shown in Fig. 2 B, E, and F, respectively. The model predicts that free energy is lowered along  $N_I U_{II} \rightarrow N_I N_{II}$  by 5 to  $10k_B T$  than  $U_I U_{II} \rightarrow U_I N_{II}$ , and therefore  $P_I$  becomes more favored to make  $N_I U_{II}$  the intermediate. In this case, it is expected that the mutations that weaken the domain–domain interactions do not significantly affect the folding rate of domain I although they lower the folding rate of domain II.

**Protein S.** *Mycococcus xanthus* spore coat protein S is a 173-aa protein. As shown in Fig. 4A, protein S has two domains, each of which consists of Greek-key motifs (PDB ID: 1PRS). The overall structure of protein S is, therefore, similar to that of H $\gamma$ D-Crys (23, 24), but protein S has different structural features. Domain–domain interactions are formed mainly between Cth-I and Nth-II. From this structural pattern, we expect that the domain–domain interactions are stabilized when the region from Cth-I through Nth-II becomes native-like. This topological constraint suggests no preference of order of folding of the two domains. There are, however, minor inhomogeneities in distributions of domain–domain interactions arising from interactions between Nth-I and Nth-II in the native conformation.

Also shown in Fig. 4 are  $F(x, y)$  for  $\epsilon/k_B T = 0.58$  (Fig. 4B), the corresponding  $U(x, y)$  (Fig. 4D), and  $F_0(x, y)$  (Fig. 4C), where we assume  $n_I = 87$  and  $n_{II} = 86$ . As in H $\gamma$ D-Crys,  $F(x, y)$  of protein S has distinct minima at  $N_I N_{II}$ ,  $U_I N_{II}$ ,  $N_I U_{II}$ , and  $U_I U_{II}$ , and two pathways  $P_I$  and  $P_{II}$  connecting them are possible. As is expected from the above topological consideration, the free energy profile along  $P_I$  and that along  $P_{II}$  are not significantly different.  $U(x, y)$  has the large negative values at the native state and at  $(50 < x < 87, 50 < y < 86)$ , which lowers the free energy barrier height of both  $P_I$  and  $P_{II}$ . Corresponding to the minor distributions of interactions between Nth-I and Nth-II, however, the region in which  $U(x, y)$  takes low values is wider for  $x > y$  than the region for  $x < y$ . Owing to this asymmetrical free energy lowering, the model predicts that  $P_I$  that passes  $N_I U_{II}$  should have a larger folding rate than  $P_{II}$ .

**R1617 Spectrin Domain.** As shown in Fig. 5A, each spectrin domain consists of three helices A, B, and C, so helix C of domain I forms a continuous helix with helix A of domain II. Pairs of spectrin domains connected in this way are significantly more stable than the isolated separated domains (26). We here study the connected pair of R16 and R17 (R1617, PDB ID: 1CUN) by truncating 7 residues from the C terminus of 1CUN. Although the folding intermediate does not exist in equilibrium, kinetic analyses showed that domain I (R16) folds first and is followed by domain II (R17) (28). Thus, R1617 shows cooperative folding despite the small number of residues that form the domain–domain interactions.

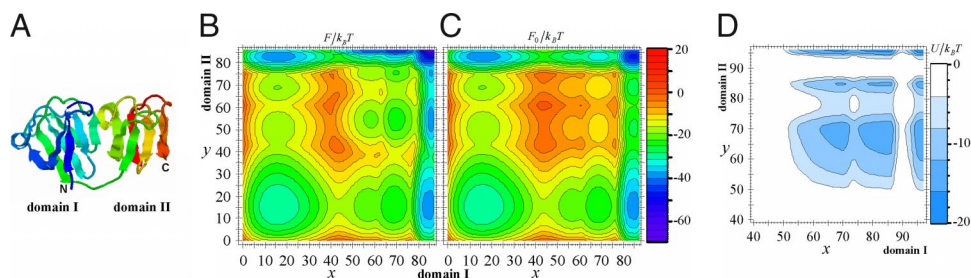


**Fig. 4.** Structure and free energy profiles of protein S. (A) Structure of protein S (PDB ID: 1PRS). Shown are  $F(x, y)$  (B),  $F_0(x, y)$  (C), and  $U(x, y)$  (D) for  $\epsilon/k_B T = 0.58$ .

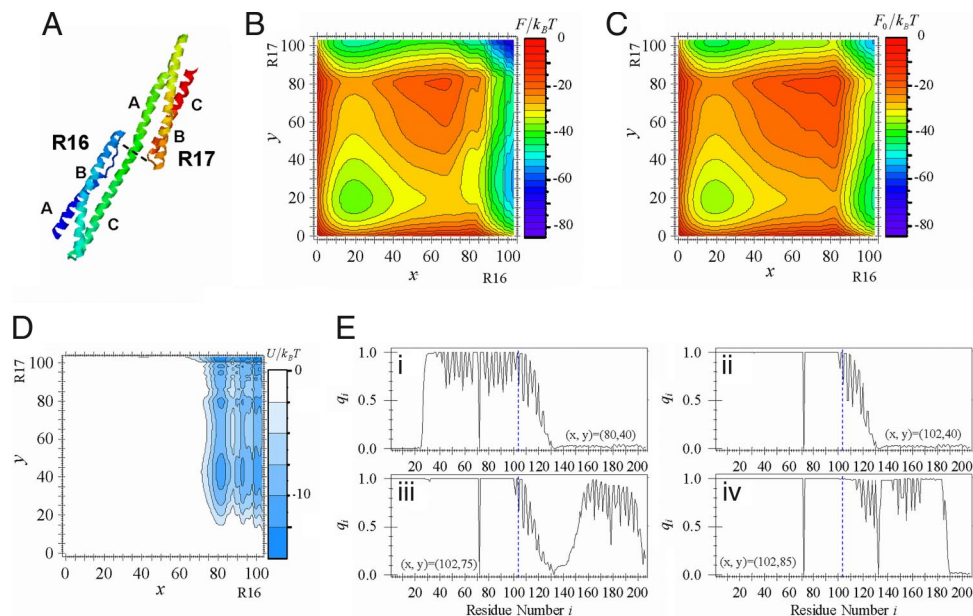


**Fig. 5.** Structure and free energy profiles of the R1617 spectrin domain. (A) structure of R1617 (PDB ID: 1CUN). Each domain consists of three helices A, B, and C. Shown are  $F(x, y)$  (B),  $F_0(x, y)$  (C), and  $U(x, y)$  (D) for  $\varepsilon/k_B T = 0.6$ . Structural order parameters  $q_i(x, y)$  for each residue are  $(x, y) = (80, 40)$  (Ei),  $(x, y) = (102, 40)$  (Eii),  $(x, y) = (102, 75)$  (Eiii), and  $(x, y) = (102, 85)$  (Eiv).

By assuming  $n_I = 103$  and  $n_{II} = 103$ ,  $F(x, y)$ ,  $F_0(x, y)$ , and  $U(x, y)$  of R1617 for  $\varepsilon/k_B T = 0.6$  are shown in Fig. 5 B, C, and D, respectively.  $F(x, y)$  has four free energy minima, so there are two pathways,  $P_I$  and  $P_{II}$ , where  $P_I$  passing  $N_I U_{II}$  traverses the surface of free energy lower than that of  $P_{II}$ . Predominance of  $P_I$  is consistent with the observed results, showing that the folding intermediate is  $N_I U_{II}$  (27, 28).  $F_0(x, y)$  has a symmetrical pattern showing that isolated domains I and II are almost identical in their folding kinetics. Asymmetry of  $P_I$  and  $P_{II}$  arises from the large negative values of  $U(x, y)$  at large  $x$ . The large negative values of  $U(x, y)$  are not found in the region of small  $x$ , which is consistent with the observed data that the folding rate of R16 in R1617 is similar to that of isolated R16 but the unfolding rate of R16 in R1617 is significantly smaller than that of isolated R16 (28).

Asymmetry of  $U(x, y)$  is due to the asymmetric domain–domain interactions. We refer to the contiguous helix connecting domains I and II as the helix C-A. Domain I consists of helix A, helix B, and the N-terminal half of helix C-A, whereas domain II consists of the C-terminal half of helix C-A, helix B, and helix C. The domain–domain interactions are formed between helix C-A and the loop connecting helices A and B of domain I and between helix C-A and the loop between helices B and C of domain II, where the number of native contacts is larger in the former interactions. Such asymmetry inevitably arises from the repeat of almost equivalent domains unless each domain has a special symmetry to allow the same interactions at different sites. With this asymmetry, as shown with  $q_i(x, y)$  of Fig. 5 E1–E4, helix B of domain I and helix C-A form first, which catalyzes the folding of the remainder of the protein, helix A of domain I and helices B and C in domain II.

**Summary and Discussion.** We examined the multidomain proteins H $\gamma$ D-Crys, protein S, and R1617 by using a structure-based, coarse-grained model of folding. The calculated results consistently explained many experimental data showing that the structure-based model captures the essential features of folding of multidomain proteins. Two domains in H $\gamma$ D-Crys interact with each other in an almost symmetrical way, but the asym-

metrical chain connectivity between the two domains determines the folding pathway and the intermediate. The model predicted that a change of the connectivity by circular permutation should change the folding pathway. In protein S, two domains are connected in an almost symmetrical way, but the domain–domain interactions are asymmetric, which should determine the relative weight of multiple folding pathways. In R1617, a helix extends from one domain to another. Although the two domains are quite similar to each other, the asymmetric interactions between this helix and the remainder of the protein determines the folding pathway and intermediate. In this way, the connectivity of the two domains and the distribution of domain–domain interactions in the native conformation are factors to determine kinetic and equilibrium properties of folding.

Folding of multidomain proteins resembles the binding of a pair or oligomer of proteins to form complexes. In complex formation, binding proceeds not only as docking of rigidly folded monomers, but there are many cases in which binding and folding occur concomitantly (42, 43). In the latter cases, binding proceeds as a two-state transition from unfolded monomers to a folded complex or via an intermediate depending on the strength of interactions between folding units (i.e., monomers) (44, 45). Also in the present multidomain cases, interactions between folding units (i.e., domains) are important, but, as shown here, the other important factor, which is absent in complex formation, is the chain connectivity between folding units.

Effects of the chain connectivity and the distribution pattern of domain–domain interactions are reflected in the functional form of  $U(x, y)$  in the model. In the present model, large cancellation between enthalpy and entropy is already taken into account in calculation of  $F_0(x, y)$ , so that  $U(x, y)$ , which is determined by the residual domain–domain interactions and the connectivity, decisively controls the catalytic effect on the folding process and the subtle balance between multiple possible pathways. Although  $F_0(x, y)$  depends on the parameters in the model or on the precise definition of native pairs, the overall functional form of  $U(x, y)$  is insensitive to changes in these details. We conclude, therefore, that the topology of the native conformation is the primary determinant of the folding and un-

folding processes of multidomain proteins. This theoretical conclusion should be verified by further examining different multidomain proteins. Especially interesting would be the examination of artificially designed homodimers connected by linkers.

The present results suggest that the functionally important features of multidomain proteins can be controlled by the topological design: Design of the chain connectivity and the distribution of domain–domain interactions should determine the structural features of folding intermediates and determine which domain is more unstable, which may be relevant to the functional requirements of proteins. This design principle should be useful in protein engineering and in analyzing the evolutionary history of proteins in a family or a superfamily. Combined efforts with the coarse-grained, structure-based models, all-atom simulations, and experiments should help to examine the design principle proposed in this article.

## Methods

In the present model, we define  $\Delta_{ij} = 1$  when a heavy atom other than hydrogen in the  $i$ th residue and a heavy atom in the  $j$ th residue with  $j > i + 2$

are closer than 5 Å in the native conformation and  $\Delta_{ij} = 0$  otherwise. Throughout this article we use  $\sigma = 1.5k_B$  ( $\nu \approx 4.5$ ), but independence of  $U(x, y)$  on  $\sigma$  assures the insensitivity of the effects of domain–domain interactions to the choice of the precise value of  $\sigma$ .  $F(x, y)$  for  $\sigma \neq 1.5k_B$  can be obtained by using the free energy function at  $\sigma = 1.5k_B$  as  $F(x, y) = F(x, y)|_{\sigma = 1.5k_B} + T(N - x - y)(\sigma - 1.5k_B)$ .

Response to the perturbation of interactions with respect to the  $i$ th residue,  $q_i(x, y)$ , is defined as follows: When the strength of interactions that involve the  $i$ th residue is changed from  $\varepsilon$  to  $\varepsilon + \Delta\varepsilon$ , then energy is modulated as  $\Delta H(i) = \Delta\varepsilon \sum_j \Delta_{ij} m_{ij}$ .  $q_i(x, y)$  is defined by  $q_i(x, y) = \Delta F_i(x, y) / \Delta\varepsilon \sum_j \Delta_{ij}$  with  $\Delta F_i(x, y) = -k_B T \ln(\exp[-\beta \Delta H(i)]_{x,y})$ . From this definition, we can see that  $q_i(x, y)$  is normalized to be  $0 \leq q_i(x, y) \leq 1$ . At the transition state region of  $(x, y)$ ,  $q_i(x, y)$  provides information similar to the  $\Phi$  value (10). Also, in other regions of  $(x, y)$ ,  $q_i(x, y)$  can be used as an order parameter to represent the native-likeness of the  $i$ th site under the constraint of  $(x, y)$ .

**ACKNOWLEDGMENTS.** This work was supported by grants from the Ministry of Education, Culture, Sports, Science, and Technology, Japan, and by grants for the 21st century Center of Excellence program for Frontiers of Computational Science.

- Onuchic JN, Luthey-Schulten Z, Wolynes PG (1997) Theory of protein folding: The energy landscape perspective. *Annu Rev Phys Chem* 48:545–600.
- Fersht A (1999) *Structure and Mechanism in Protein Sci: A Guide to Enzyme Catalysis and Protein Folding* (Freeman & Company, New York).
- Onuchic JN, Wolynes PG (2004) Theory of protein folding. *Curr Opin Struct Biol* 14:70–75.
- Das P, Matysiak S, Clementi C (2005) Balancing energy and entropy: A minimalist model for the characterization of protein folding landscapes. *Proc Natl Acad Sci USA* 102:10141–10146.
- Hubner IA, Deeds EJ, Shakhnovich EI (2006) Understanding ensemble protein folding at atomic detail. *Proc Natl Acad Sci USA* 103:17747–17752.
- Li L, Shakhnovich EI (2001) Constructing, verifying, and dissecting the folding transition state of chymotrypsin inhibitor 2 with all-atom simulations. *Proc Natl Acad Sci USA* 98:13014–13018.
- Clementi C, Garcia AE, Onuchic JN (2003) Interplay among tertiary contacts, secondary structure formation and side-chain packing in the protein folding mechanism: An all-atom representation study. *J Mol Biol* 326:933–954.
- Papoian GA, Ulander J, Eastwood MP, Luthey-Schulten Z, Wolynes PG (2004) Water in protein structure prediction. *Proc Natl Acad Sci USA* 101:3352–3357.
- Karanicolas J, Brooks CL (2002) The origins of asymmetry in the folding transition states of protein L and protein G. *Protein Sci* 11:2351–2361.
- Itoh K, Sasai M (2006) Flexibly varying folding mechanism of a nearly symmetrical protein: B domain of protein A. *Proc Natl Acad Sci USA* 103:7298–7303.
- Han JH, Batey S, Nickson AA, Teichmann SA, Clarke J (2007) The folding and evolution of multidomain proteins. *Nat Rev Mol Cell Biol* 8:319–330.
- Kamagata K, Arai M, Kuwajima K (2004) Unification of the folding mechanisms of non-two-state and two-state proteins. *J Mol Biol* 339:951–965.
- Ferreiro DU, Cho SS, Komives EA, Wolynes PG (2005) The energy landscape of modular repeat proteins: Topology determines folding mechanism in the ankyrin family. *J Mol Biol* 354:679–692.
- Barrick D, Ferreiro DU, Komives EA (2008) Folding landscapes of ankyrin repeat proteins: Experiments meet theory. *Curr Opin Struct Biol* 18:27–34.
- Ferreiro DU, Walczak AM, Komives EA, Wolynes PG (2008) The energy landscapes of repeat-containing proteins: Topology, cooperativity, and the folding funnels of one-dimensional architectures. *PLoS Comput Biol* 4:e1000070.
- Cho SS, Levy Y, Wolynes PG (2006) P versus Q: Structural reaction coordinates capture protein folding on smooth landscapes. *Proc Natl Acad Sci USA* 103:586–591.
- Kosinski-Collins MS, King J (2003) In vitro unfolding, refolding, and polymerization of human  $\gamma$ D crystallin, a protein involved in cataract formation. *Protein Sci* 12:480–490.
- Kosinski-Collins MS, Flaugh SL, King J (2004) Probing folding and fluorescence quenching in human  $\gamma$ D crystallin Greek key domains using triple tryptophan mutant proteins. *Protein Sci* 13:2223–2235.
- Flaugh SL, Kosinski-Collins MS, King J (2005) Contributions of hydrophobic domain interface interactions to the folding and stability of human  $\gamma$ D-crystallin. *Protein Sci* 14:569–581.
- Flaugh SL, Kosinski-Collins MS, King J (2005) Interdomain side-chain interactions in human  $\gamma$ D crystallin influencing folding and stability. *Protein Sci* 14:2030–2043.
- Flaugh SL, Mills IA, King J (2006) Glutamine deamidation destabilizes human  $\gamma$ D-crystallin and lowers the kinetic barrier to unfolding. *J Biol Chem* 281:30782–30793.
- Mills IA, Flaugh SL, Kosinski-Collins MS, King J (2007) Folding and stability of the isolated Greek key domains of the long-lived human lens proteins  $\gamma$ D-crystallin and  $\gamma$ S-crystallin. *Protein Sci* 16:2427–2444.
- Wenk M, Mayr EM (1998) *Myxococcus xanthus* spore coat protein S, a stress-induced member of the  $\beta$ - $\gamma$ -crystallin superfamily, gains stability from binding of calcium ions. *Eur J Biochem* 255:604–610.
- Wenk M, Jaenicke R, Mayr EM (1998) Kinetic stabilization of a modular protein by domain interactions. *FEBS Lett* 438:127–130.
- MacDonald RI, Pozharski EV (2001) Free energies of urea and of thermal unfolding show that two tandem repeats of spectrin are thermodynamically more stable than a single repeat. *Biochemistry* 40:3974–3984.
- Scott KA, Batey S, Hooton KA, Clarke J (2004) The folding of spectrin domains I: Wild-type domains have the same stability but very different kinetic properties. *J Mol Biol* 344:195–205.
- Batey S, Randles LG, Steward A, Clarke J (2005) Cooperative folding in a multi-domain protein. *J Mol Biol* 349:1045–1059.
- Batey S, Scott KA, Clarke J (2006) Complex folding kinetics of a multidomain protein. *Biophys J* 90:2120–2130.
- Wako H, Saito N (1978) Statistical mechanical theory of protein conformation 1. General considerations and application to homopolymers. *J Phys Soc Jpn* 44:1931–1938.
- Wako H, Saito N (1978) Statistical mechanical theory of protein conformation 2. Folding pathway for protein. *J Phys Soc Jpn* 44:1939–1945.
- Go N, Abe H (1981) Noninteracting local-structure model of folding and unfolding transition in globular proteins. I. Formulation. *Biopolymers* 20:991–1011.
- Muñoz V, Eaton WA (1999) A simple model for calculating the kinetics of protein folding from three-dimensional structures. *Proc Natl Acad Sci USA* 96:11311–11316.
- Henry ER, Eaton WA (2004) Combinatorial modeling of protein folding kinetics: Free energy profiles and rates. *Chem Phys* 307:163–185.
- Bruscolini P, Pelizzola (2002) A Exact solution of the Muñoz–Eaton model for protein folding. *Phys Rev Lett* 88:258101.
- Zamparo M, Pelizzola (2006) A Kinetics of the Wako–Saitō–Muñoz–Eaton model of protein folding. *Phys Rev Lett* 97:068106.
- Bruscolini P, Pelizzola A, Zamparo M (2007) Rate determining factors in protein model structures. *Phys Rev Lett* 99:038103.
- Nelson ED, Grishin NV (2008) Folding domain B of protein A on a dynamically partitioned free energy landscape. *Proc Natl Acad Sci USA* 105:1489–1493.
- Imparato A, Pelizzola A, Zamparo M (2007) Ising-like model for protein mechanical unfolding. *Phys Rev Lett* 98:148102.
- Itoh K, Sasai M (2004) Dynamical transition and proteinquake in photoactive yellow protein. *Proc Natl Acad Sci USA* 101:14736–14741.
- Clementi C, Jennings PA, Onuchic JN (2001) Prediction of folding mechanism for circular-permuted proteins. *J Mol Biol* 311:879–890.
- Hubner IA, Lindberg M, Haglund E, Oliveberg M, Shakhnovich EI (2006) Common motifs and topological effects in the protein folding transition state. *J Mol Biol* 359:1075–1085.
- Papoian GA, Wolynes PG (2003) The physics and bioinformatics of binding and folding—an energy landscape perspective. *Biopolymers* 68:333–349.
- Terada TP, Sasai M, Yomo T (2002) Conformational change of actomyosin complex drives the multiple stepping movement. *Proc Natl Acad Sci USA* 99:9202–9206.
- Levy Y, Wolynes PG, Onuchic JN (2004) Protein topology determines binding mechanism. *Proc Natl Acad Sci USA* 101:511–516.
- Levy Y, Cho SS, Onuchic JN, Wolynes PG (2005) A survey of flexible protein binding mechanisms and their transition states using native topology based energy landscapes. *J Mol Biol* 346:1121–1145.